Future Vehicle Driven by Electricity and Control—Research on Four-Wheel-Motored "UOT Electric March II"

Yoichi Hori, *Senior Member, IEEE*

***Abstract*—The electric vehicle (EV) is the most exciting object to apply "advanced motion control" technique. As an EV is driven by electric motors, it has the following three remarkable advantages: 1) motor torque generation is fast and accurate; 2) motors can be installed in two or four wheels; and 3) motor torque can be known precisely. These advantages enable us to easily realize: 1) high performance antilock braking system and traction control system with minor feedback control at each wheel; 2) chassis motion control like direct yaw control; and 3) estimation of road surface condition. "UOT Electric March II" is our novel experimental EV with four in-wheel motors. This EV is made for intensive study of advanced motion control of an EV.**

***Index Terms*—Adhesion control, antilock braking system (ABS), body slip angle estimation, direct yaw control (DYC), electric vehicle (EV), estimation of road surface condition, motion control, slip ratio control (SRC), traction control system (TCS).**

I. Three Advantages of Electric Vehicle

RECENTLY, pure electric vehicles (PEVs) have achieved sufficient driving performance thanks to drastic improvements in motors and batteries. On the other hand, hybrid EVs (HEVs), like the Toyota Prius, will be widely used in the next ten years. Fuel-cell vehicles (FCVs) will be the major vehicles in the 21st century. Such development has the strong incentives of energy efficiency and global environmental protection.

However, it is not well recognized that the most distinct advantage of the EV is the quick and precise torque generation of the electric motor. If we do not utilize this merit, the EV will never be used in the future. For example, if a diesel HEV is developed, its energy consumption will be extremely low. The EV cannot compete against such vehicles in terms of energy efficiency or CO_2 emissions. On the contrary, if we recognize the advantage of the EV in control performance and succeed in the development of new concept vehicles, a bright future will be waiting for us.

We can summarize the advantages of the EV into the following three points.

1) *Torque generation of an electric motor is very quick and accurate.*

   This is the essential advantage. The electric motor's torque response is several milliseconds, 10–100 times as fast as that of the internal combustion engine or hydraulic braking system. This enables feedback control and we can change vehicle characteristics without any change in characteristics from the driver. This is exactly based on the concept of a two-degrees-of-freedom (2DOF) control system. A "Super Antilock Brake System (ABS)" will be possible. Moreover, an ABS and traction control system (TCS) can be integrated, because a motor can generate both acceleration or deceleration torques. If we can use low-drag tires, it will greatly contribute to energy saving.
2) *A motor can be attached to each wheel.*

   Small but powerful electric motors installed into each wheel can generate even the antidirectional torques on left and right wheels. Distributed motor location can enhance the performance of Vehicle Stability Control (VSC) such as Direct Yaw Control (DYC). It is not permitted for an Internal Combustion engine Vehicle (ICV) to use four engines, but it is all right to use four small motors without a big cost increase.
3) *Motor torque can be measured easily.*

   There is much smaller uncertainty in driving or braking torque generated by an electrical motor, compared to that of an IC engine or hydraulic brake. It can be known from the motor current. Therefore, a simple "driving force observer" can be designed and we can easily estimate the driving and braking force between tire and road surface in real time. This advantage will contribute greatly to application of new control strategies based on road condition estimation. For example, it will be possible to alert the driver, "We have now entered a snowy road!"

These advantages of the electric motor will open the new possibility of novel vehicle motion control for electric vehicles. Our final target is to realize a novel vehicle control system with four independently controlled in-wheel motors, as depicted in Figs. 1 and 2. It shows the integrated system with "minor feedback control loop at each wheel" and "total chassis controller" as an outer weak feedback loop. Here, Model-Following Control (MFC) is drawn as an example of the minor loop. A very short time delay is required for the actuator to perform such effective feedback controls.

II. What Can We Do With an EV?

As examples of novel control techniques, which can be realized primarily in EVs, we are investigating several techniques.

Manuscript received November 4, 2002; revised April 29, 2004. Abstract published on the Internet July 15, 2004.

The author is with the Institute of Industrial Science, The University of Tokyo, Tokyo 153-8505, Japan (e-mail: hori@iis.u-tokyo.ac.jp).

Digital Object Identifier 10.1109/TIE.2004.834944

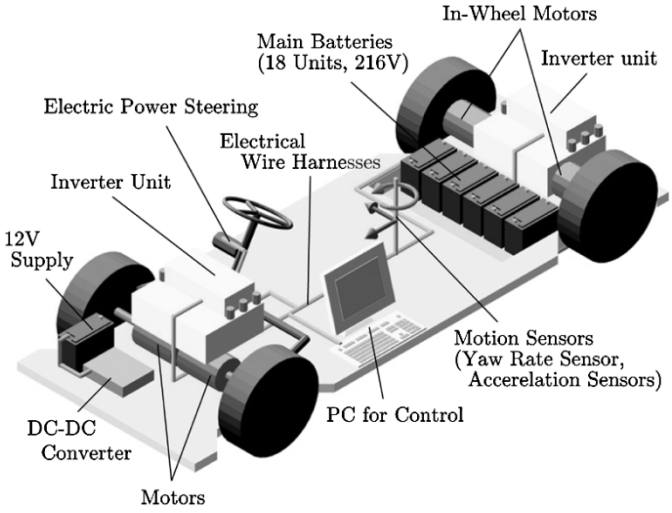

Fig. 1. Sketch of "UOT March II."

TABLE I
SPECIFICATIONS OF "UOT ELECTRIC MARCH II"

Drivetrain	**4 PM Motors / Meidensya Co.**
Max. Power(20 sec.)	36 [kW] (48.3[HP])*
Max. Torque	77* [Nm]
Gear Ratio	5.0
Battery	**Lead Acid**
Weight	14.0 [kg](for 1 unit)
Total Voltage	228 [V] (with 19 units)
Base Chassis	**Nissan March K11**
Wheel Base	2360 [m]
Wheel Tread F/R	1365/1325 [m]
Total Weight	1400 [kg]
Wheel Inertia**	8.2 [kg]***
Wheel Radius	0.28 [m]
Controller	
CPU	MMX Pentium 233[MHz]
Rotary Encoder	3600 [ppr]***
Gyro Sensor	Fiber Optical Type

* ... for only one motor. ** ... mass equivalent.
*** ... affected by gear ratio.

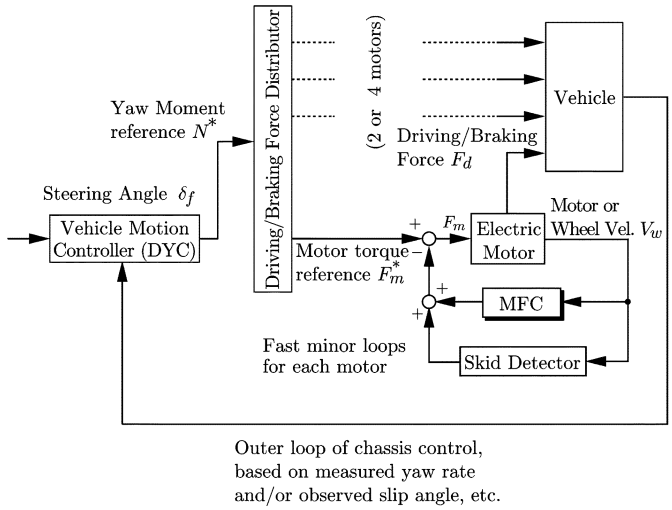

Fig. 2. Control system to be realized in "UOT March II."

A. Adhesion Control of Tire and Road Surface

In this control method, the advantage of an electric motor is most effectively utilized:

1) MFC;
2) Slip Ratio Control (SRC);
3) cooperation with higher level control like DYC;
4) wheel skid detection without vehicle speed knowledge.

B. High-Performance Braking Control

We can realize a higher performance braking control system like an elevator utilizing an electric motor's controllability:

1) pure electric braking control in a whole speed range;
2) hybrid ABS for HEV; fast but small torque electric brake can assist hydraulic brake system, which has big torque but slow response;
3) direct control of driving force at each tire.

C. Two-Dimensional Attitude Control

The aim of two-dimensional attitude control is basically to find the solution to the problem of how to mix the controls of γ (yaw rate) and β (body slip angle). It consists of linearization of transfer characteristic from driver's angle δ_f to γ and control β to be zero:

1) decoupling control of β and γ;
2) higher performance coordination of Active Front Steering (AFS) and DYC;
3) vehicle dynamics control based on β estimation;
4) dynamic driving force distribution considering side force and cooperation with suspension system under changing load.

D. Road Surface Condition Estimation

As the motor torque can be known easily from the motor current, we can apply various kinds of estimation techniques:

1) estimation of gradient of μ–λ curve;
2) estimation of the maximum friction coefficient;
3) estimation of the optimal slip ratio to be used for SRC;
4) higher performance DYC based on the estimation of road surface condition.

III. NOVEL EXPERIMENTAL ELECTRIC VEHICLE "UOT MARCH II"

Our EV "UOT (University of Tokyo) Electric March II" was constructed in 2001. The most remarkable feature of this EV is the in-wheel motor mounted in each wheel. We can control each wheel torque completely and independently. Regenerative braking is, of course, available. We built this EV ourselves by remodeling a Nissan March.

Table I lists the specifications of the "UOT Electric March II." It uses a permanent-magnet (PM) motor and has a built-in drum brake and reduction gear. The motor unit is as compact as the wheel. Two motors are placed at the ends of each driving shaft, and attached to the base chassis as shown in Fig. 3(a) and (d). The electric motors are controlled by on-board personal computers (PCs).

We use another PC for motion control. They are connected to several sensors, such as, a fiber-optical gyro sensor, three-axis acceleration sensor, and so on. A motion controller is installed

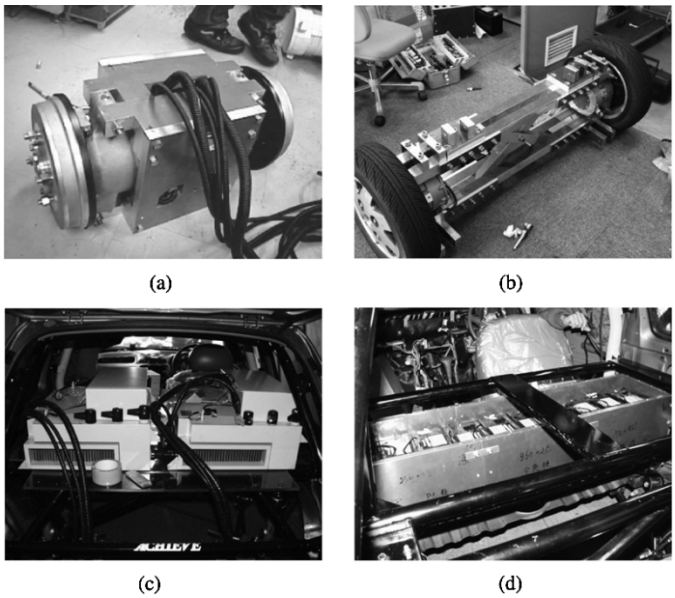

Fig. 3. Main parts of UOT Electric March II. (a) Front motors. (b) Rear motors. (c) Inverters. (d) Batteries.

in the second PC. It outputs the motor torque references, and two inverter units generate the required motor torques. Precise torque generation is achieved by the motor current controller in the inverter units. In order to detect steering angle, the encoder signal for EPS is used.

IV. Antiskid Control in Longitudinal Direction

In this section, a wheel controller for skid prevention is proposed. The starting point of this idea is to utilize the knowledge obtained in advanced motion control techniques of electric motors. Generally speaking, a feedback controller can change mechanical plant dynamics. For example, the plant can be insensitive to disturbance if an appropriate feedback controller is applied. Fast response of the actuator, which is readily available in an EV, can realize such controls. We propose two anti-slip controllers: MFC and SRC.

A. MFC

In the simple model of one wheel shown in Fig. 4, the slip ratio λ is given by

$$\lambda = \frac{V_w - V}{\max(V_w, V)} \tag{1}$$

where V is the vehicle chassis velocity, and V_w is the wheel velocity given by $V_w = r\omega$. r and ω are the wheel radius and rotational velocity, respectively.

Fig. 5 shows the block diagram of MFC. F_m^* is the acceleration command roughly proportional to the acceleration pedal angle. $F_m^* = T^* r$, where T^* is the driver's command torque. ω increases drastically when the tire slips.

Vehicle dynamics including tire and road surface characteristics are very complicated, but if we use the slip ratio λ, the

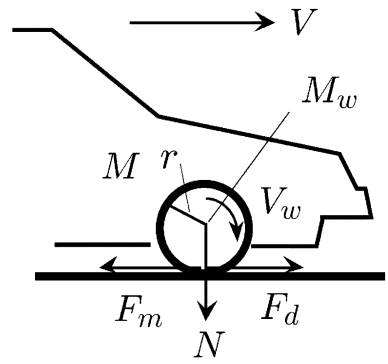

Fig. 4. One wheel model.

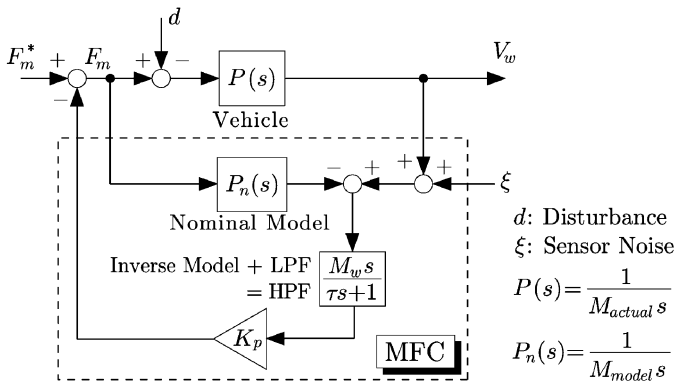

Fig. 5. Block diagram of the proposed feedback controller "MFC."

vehicle body can be seen as one inertia system with the equivalent inertia moment given by

$$M_{\text{actual}} \simeq M_w + M(1-\lambda). \tag{2}$$

Here, M_{actual}, M_w, and M are the total equivalent mass, wheel mass. and equivalent vehicle mass. Equation (2) means that the vehicle seems lighter when the tire slips and λ increases. We used $M_{\text{model}} = M_w + M$ with $\lambda = 0$ as the reference model.

When there is no slip, M_{actual} is almost equal to M_{model}. No control signal is generated from the MFC controller. If the tire slips, actual speed ω increases quickly. Model speed does not increase. Hence, by feeding back the speed difference to motor current command, the motor torque is reduced quickly and it induces re-adhesion.

As this control function is needed only in relatively higher frequency region, a high-pass filter with time constant τ is used on the feedback path.

When a vehicle starts skidding, the wheel velocity changes rapidly. For example, if a vehicle starts skidding during acceleration, its wheel velocity increases rapidly, and during deceleration, it decreases rapidly due to the wheel lock. Such rapid change of wheel velocity is observed as a sudden drop of wheel inertia moment. Based on this viewpoint, we design the MFC as shown in Fig. 5. Using (3) as the nominal model inertia, this controller can suppress sudden drop of inertia. Applying this controller, the dynamics of the skidding wheel becomes closer to that of the adhesive wheel.

Experiments were carried out with "UOT March-I", which is our first laboratory-made EV constructed in 1997. To simulate

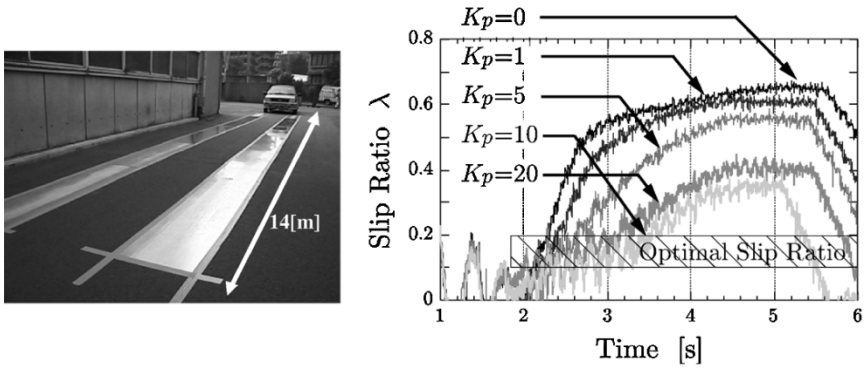

Fig. 6. Experimental results of MFC for skid prevention with $\tau = 0.1$.

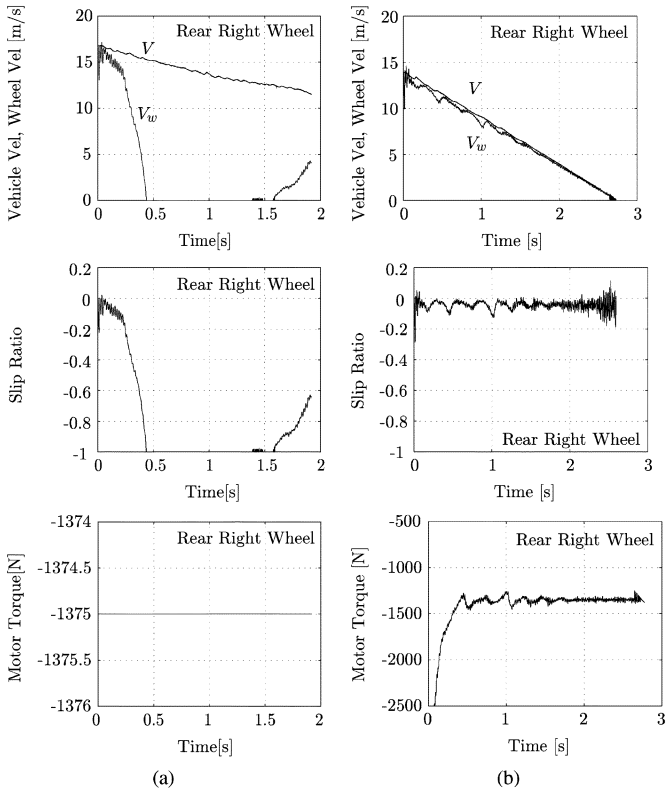

Fig. 7. Results of rapid braking experiment. (a) Without MFC. (b) With MFC.

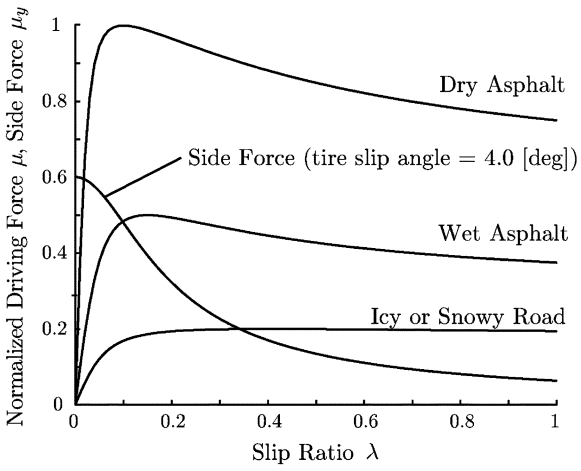

Fig. 8. Typical μ–λ curve.

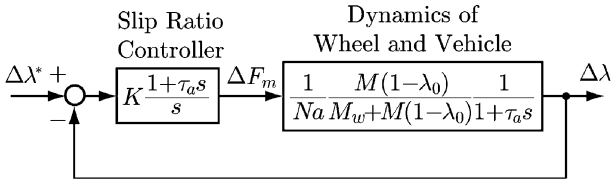

Fig. 9. Slip ratio controller.

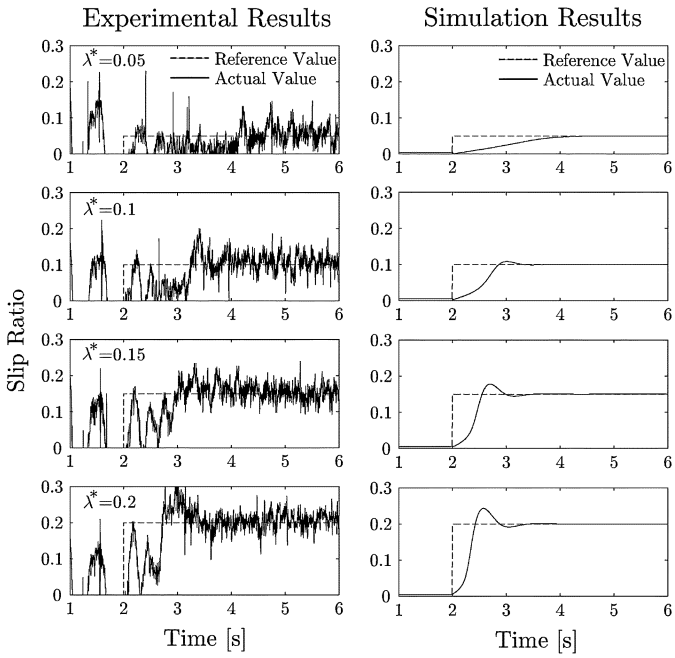

Fig. 10. Experimental results of SRC.

a slippery low-μ road, we put aluminum plates of 14-m length on the asphalt, and spread water on them. The peak μ of this test road was estimated at about 0.5.

Fig. 6 shows the time responses of slip ratio. In these experiments, the vehicle was accelerated on the slippery test road, while the motor torque was increased linearly. Without control, the slip ratio rapidly increases. On the contrary, the increase of slip ratio is suppressed when the proposed controller is applied.

Fig. 7 shows the experimental results using "UOT March II" on a professional test course. The car is decelerated suddenly on the slippery course, where $\mu_{\rm peak}$ was about 0.5. Without control, the wheel velocity rapidly decreased and the vehicle's wheels

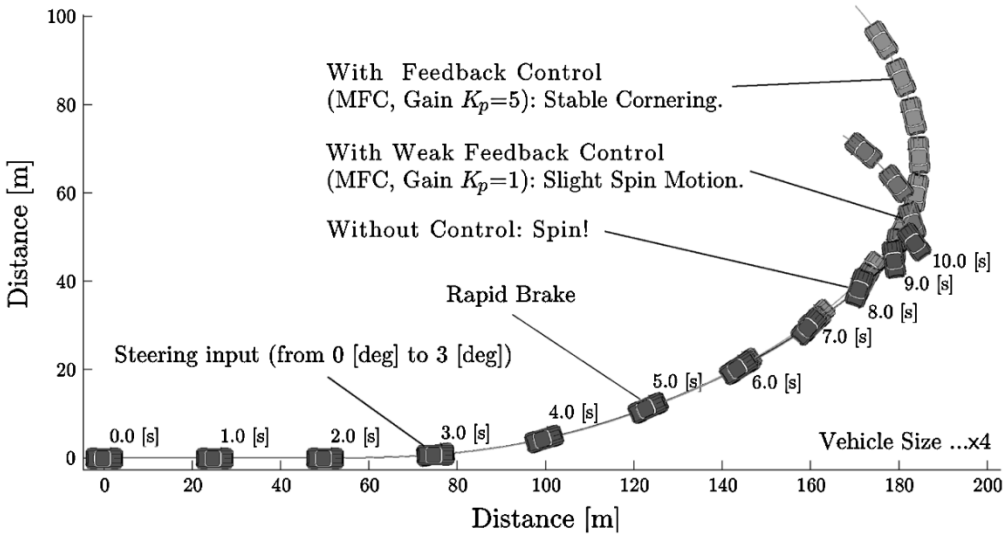

Fig. 11. Stabilizing effect with controlled four wheels is visualized with vehicle trajectory (rapid brake during curve turning, on a slippery road).

were soon locked as seen in Fig. 7(a). In contrast, when MFC is applied, the wheels were not locked, and the vehicle stopped safely [Fig. 7(b)].

B. SRC

MFC showed that electric motor control can change mechanical characteristics. If we need more exactly to regulate the slip ratio within a specified range, a more precise approach is necessary.

Based on the tire model shown in Fig. 4, under some practical assumptions, the kinetic equations of the wheel and vehicle take the forms of

$$(F_m - F_d)\frac{1}{M_w s} = V_w \tag{3}$$

$$F_d \frac{1}{Ms} = V. \tag{4}$$

The friction force between the road and the wheel is given by

$$F_d = N\mu(\lambda) \tag{5}$$

where F_m is the motor torque (force equivalent), F_d the friction force, M_w the wheel inertia (mass equivalent), M the vehicle weight, and N the vertical force given by $N = Mg$. Fig. 8 gives the typical characteristics of a μ–λ curve.

From (1), when $V_w \gg V$, the perturbation system is given by

$$\begin{aligned}\Delta\lambda &= \frac{\partial\lambda}{\partial V}\Delta V + \frac{\partial\lambda}{\partial V_w}\Delta V_w \\ &= -\frac{1}{V_{w0}}\Delta V + \frac{V_0}{V_{w0}^2}\Delta V_w\end{aligned} \tag{6}$$

where V_{w0} and V_0 are the wheel and vehicle speeds at a certain operational point. The frictional force is given by a, the gradient of μ-λ curve. a is defined by

$$\Delta\mu = a\Delta\lambda. \tag{7}$$

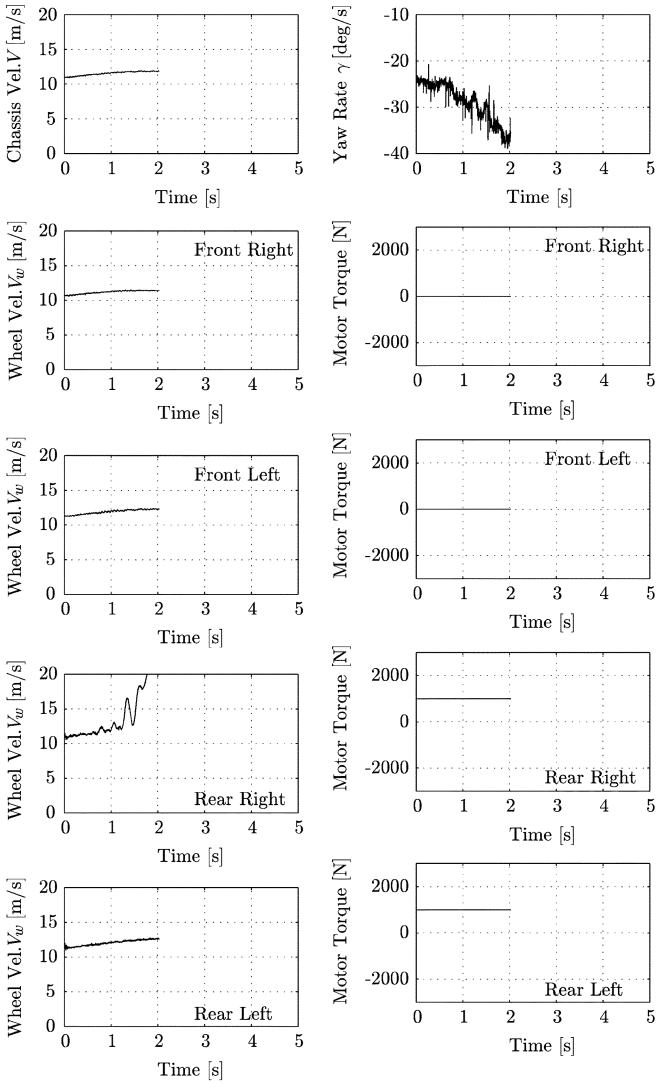

Fig. 12. Unstable cornering with sudden acceleration without MFC.

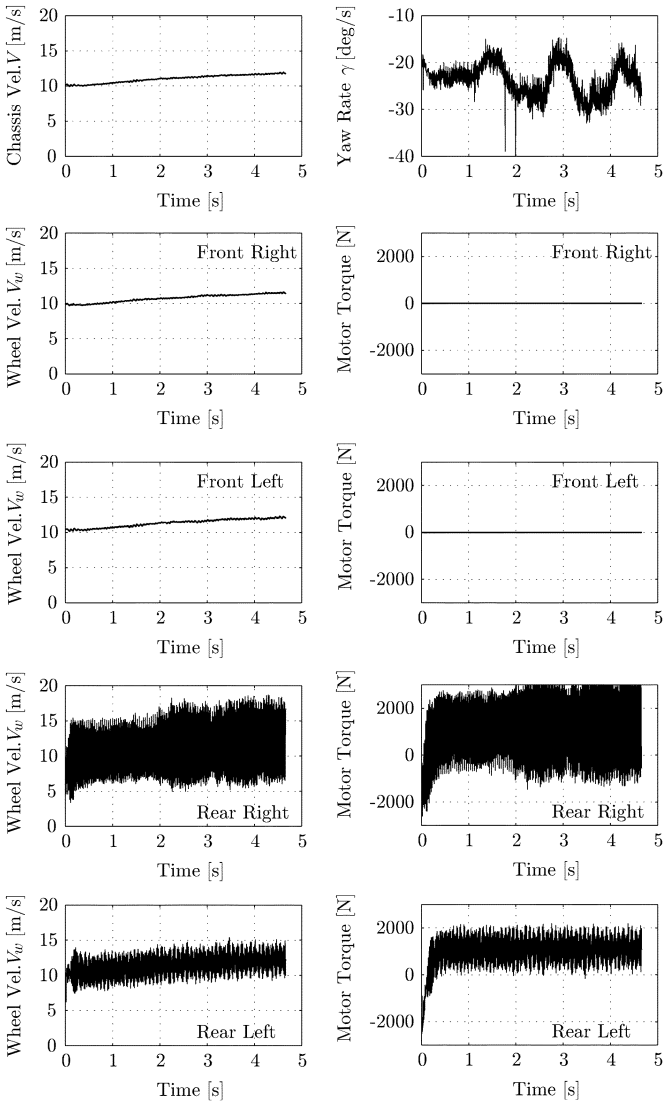

Fig. 13. Vehicle stabilizing effect of our proposed controller MFC.

The transfer function from motor torque to slip ratio is obtained by

$$\frac{\Delta\lambda}{\Delta F_m} = \frac{1}{Na}\frac{M(1-\lambda_0)}{M_w + M(1-\lambda_0)}\frac{1}{1+\tau_a s}. \tag{8}$$

The time constant τ_a is given by (10), which is proportional to the wheel speed V_{w0}

$$\tau_a = \frac{1}{Na}\frac{MM_wV_{w0}}{M_w + M(1-\lambda_0)}. \tag{9}$$

The typical value of τ_a is 150–200 ms when $a = 1$ and the vehicle speed is around 10 km/h. a can be negative in the right-hand side of the peak of the μ-λ curve.

A simple proportional–integral (PI) controller with a variable proportional gain is enough as a slip ratio controller. It is given by (11) and drawn in Fig. 9

$$K\frac{1+\tau_a s}{s}. \tag{10}$$

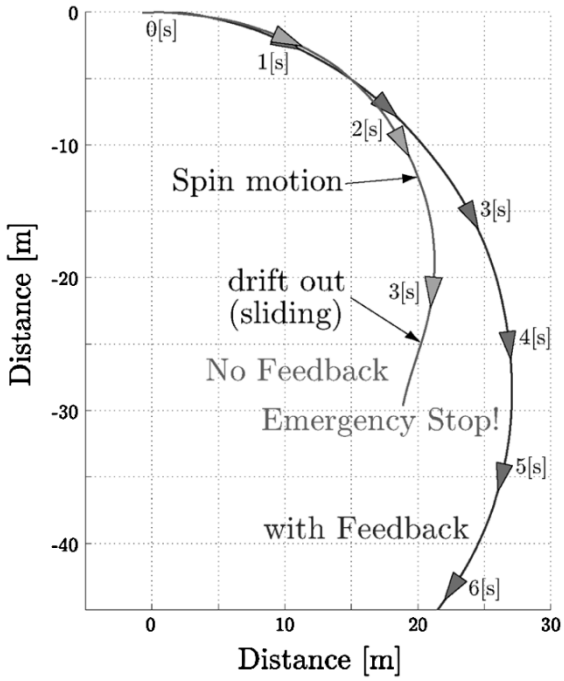

Fig. 14. Stabilizing effect of MFC installed in each wheel.

The transfer function from the slip ratio command to the actual slip ratio becomes

$$\frac{\Delta\lambda}{\Delta\lambda^*} = \frac{1}{1 + Na\frac{M_w+M(1-\lambda_0)}{M(1-\lambda_0)}\frac{1}{K}s}. \tag{11}$$

If $\lambda_0 \ll 1$, this is a simple first-order delay system with the time constant adjustable by K. Here, we put this response time at 50–100 ms.

Fig. 10 shows the experimental results of SRC using "UOT March I" and the corresponding simulations. Here, the target slip ratio is changed stepwise from 0 to various values. We can see good performance in all cases.

V. Lateral Motion Stabilization

A. Vehicle Behavior Simulation With MFC in Each Wheel

In the previous section, the minor feedback control at each wheel was discussed. Next, our interest is in what will happen if we apply such feedback control to every wheel when the vehicle is turning on a slippery road.

Here we assume that an in-wheel motor is independently attached on every wheel, and MFC is applied to each of them. The simulation results (Fig. 11) show that this minor loop can enhance the lateral stability effectively. In simulations, the chassis's 3DOF nonlinear motion dynamics, four wheels' rotation, and dynamic load distribution are also carefully considered.

The vehicle starts running on the slippery road where $\mu_{\rm peak} = 0.5$, turning left with steering angle $\delta_f = 3$ [deg]. Then, at $t = 5.0$ s, the driver inputs rapid braking torque $F_m = -1100$N on each wheel. This torque exceeds the limit of adhesion performance. Therefore, the wheel skid occurs and the chassis starts to spin, although the driver stops braking at $t = 9.0$ s. This wheel

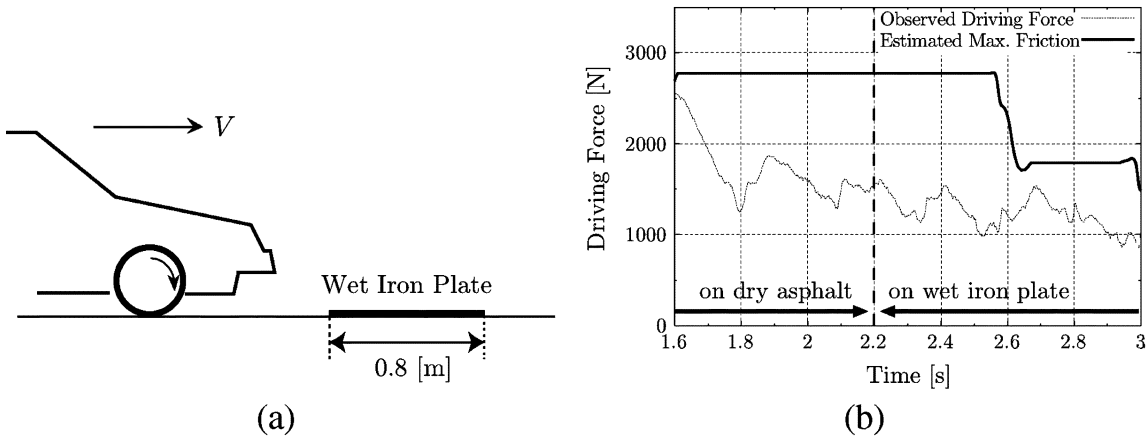

Fig. 15. Experimental results of road condition estimator. The sudden road condition change (a) was sensed with estimated maximum friction force as shown in (b).

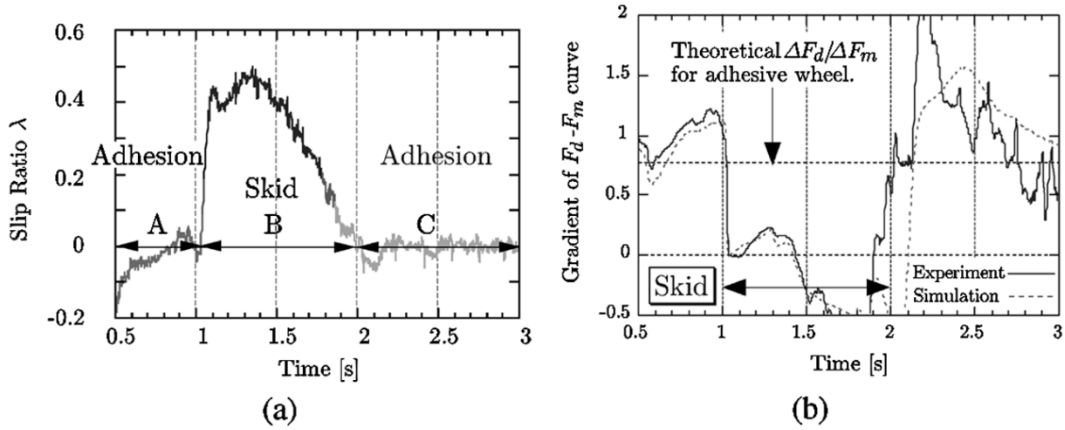

Fig. 16. Experimental results of wheel skid detector. (a) Reference slip ratio indicates that serious skid occurred during 1–2 s, and (b) the proposed method detected it.

skidding is serious, in particular, at the rear-left wheel, since the center of gravity is shifted and the load distribution changed.

On the contrary, if MFC is applied independently for each wheel, such dangerous spin motion is prevented. The rear-left wheel's torque is reduced automatically. This method MFC uses only the local wheel velocity as the feedback signal in each wheel. Therefore, it differs from conventional attitude control methods like DYC. The autonomous stabilization of lateral motion is achieved only by minor feedback control at each wheel.

B. Experiments of Stability Improvement by MFC

Next, we performed actual experiments using "UOT Electric March II" on a slippery road, known as the skid pad. The rear-wheel velocities are controlled independently by the two rear motors, though "UOT March II" has a total of four motors.

At first, "UOT March II" was turning normally in the clockwise direction. The turning radius is about 25–30 m and chassis velocity is about 40 km/h. These values are close to those of the unstable region. In these experiments, acceleration torque of 1000 N was applied to the two rear motors. Without MFC, this rapid acceleration torque causes instability as shown in Fig. 12. The rear right wheel began skidding with much danger. The yaw rate grew into the unstable region. The vehicle was in a spinning motion and completely out of control. On the contrary, as shown in Fig. 13, such dangerous vehicle motion could not be observed.

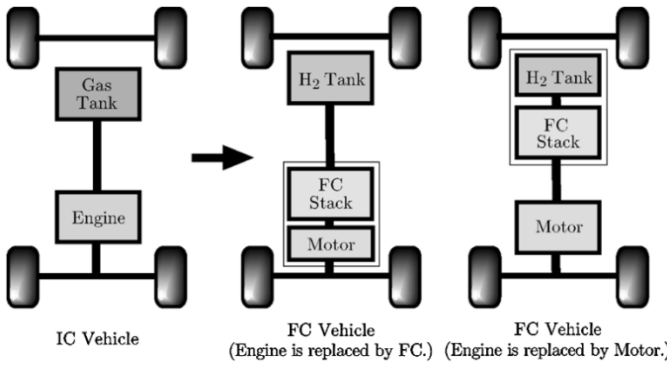

Fig. 17. Two ways to understand FCV.

Fig. 14 shows a comparison of the vehicle's trajectories. It shows that the MFC controller prevents spinout caused by excessive over steer. One of the remaining problems is the high-frequency oscillation in rear wheel torques. It can be eliminated by appropriate vibration suppression control.

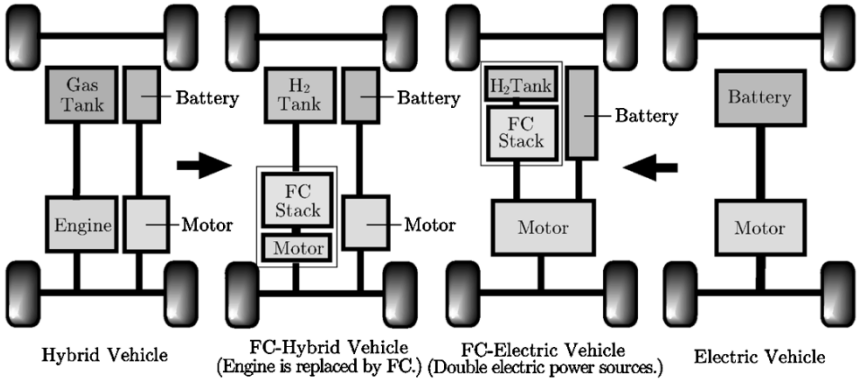

Fig. 18. Two ways to understand FCV with battery, FCHV, or FCEV?

VI. Estimation of Road Surface Condition

Some important values like slip ratio λ, body slip angle β, or road peak μ cannot be measured with practical sensors. As the motor torque can be generated precisely, its accurate value can be utilized as an information source. Estimation techniques are also important, and estimation of such variables can be easily realized in electric vehicles.

A. Road Condition Estimation

The accurate value of wheel input torque will contribute greatly to practical and precise estimation. It is available on an EV with an electric motor, but not on vehicles with combustion engines. We have proposed an estimation technique of the peak μ or maximum friction force during adhesive driving.

Fig. 15 shows the typical experimental results with UOT March I. This EV runs on the dry asphalt road, then reaches the wet iron plates. The road condition estimator calculates the maximum friction force between tire and road surface. This value indicates the sudden change of road condition, as shown in the figure. Note that even if the actual driving force is always less than the maximum frictional force, this method can still estimate maximum friction force.

This technique can be used as an alarm system to tell the driver "Please be careful. The car has now entered a slippery road!"

B. Wheel Skid Detection Without Vehicle Speed

Wheel skid detection is another application of accurate torque generation of electric motor. This method can detect the wheel skid without chassis speed measurement. As the motor torque F_m is known, driving force observer can be designed to estimate the driving force F_d, which is the friction force between the road and tire. Its principle is identical to the disturbance observer. The skid detection algorithm is very simple. When F_m increases and F_d also increases, the tire should be adhesive. When F_m increases but F_d does not increase, then it is skidding. Fig. 16 shows the experimental results using UOT March I, where we can see the validity of this method.

VII. Conclusion

In this paper, it has been pointed out that the EV is the most exciting target of advanced motion control techniques. Our novel experimental EV "UOT March II" completed in 2001 was introduced. This new four-motor EV will play an important role in our novel motion control studies of the EV. As a first attempt, we proved the effectiveness of MFC and SRC. The most remarkable point of our research is in the utilization of the electric motor's advantages: quick, accurate, and distributed torque generation.

Recent concerns for EVs are mainly focused on energy efficiency and environment, but we believe that future vehicles will be driven by electricity. If so, control is the most exciting and important topic. It is hoped that this paper will open a new field of "motion control" of electric vehicles.

Appendix
FCV—Engine Is Replaced by Electric Motor

In this appendix, the configuration of an FCV will be discussed. There are mainly two ways to understand an FCV. In Fig. 17, if we assume that the engine is replaced by an FC-stack and motor, we should compare the engine and FC-stack in various aspects, e.g., energy efficiency or power/weight ratio. On the other hand, if we assume that the gas tank is replaced by an H_2 tank and FC-stack, the engine is replaced by the motor, then we can compare the engine and the motor at various points. We are standing on this viewpoint.

Which do you think is better? We are pursuing the future possibility of the electric motor's advantage over an IC engine. An FCV uses an electric motor. Our development can be utilized in an FCV as it is. Fig. 18 shows two ways of calling an FCV. If we start from an HEV like the Toyota Prius, an FCHV is the natural name of this vehicle. The reasoning is as follows. As an FC is not enough for power generation and regenerative braking performance, an additional secondary battery and motor should be used together. In this meaning, an FCV is similar to an HEV.

On the contrary, if we understand that an FCV is simply using two types of electric power sources, the electric motor plays an important role as the main actuator. In our development of the March Project, we do not care about the kinds of energy sources. However, the usage of an electric motor is essential and crucial, because we are utilizing the advantages of the electric motor from the viewpoint of control. In this meaning, an FCV should not be called an FCHV but an FCEV.

ACKNOWLEDGMENT

The author would like to state his great appreciation to many students in the Hori Laboratory and, in particular, to Dr. S. Sakai and colleagues for their hard work and kind help in performing various experiments with the March I and II, and also to T. Okano and K. Furukawa for their help in editing the manuscript.

REFERENCES

[1] J. Ackermann, "Yaw disturbance attenuation by robust decoupling of car steering," in *Proc. 13th IFAC World Congr.*, vol. 8b-01-1, 1996, pp. 1–6.

[2] A. Daiss and U. Kiencke, "Estimation of tire slip during combined cornering and braking observer supported fuzzy estimation," in *Proc. 13th IFAC World Congress*, vol. 8b-02-2, 1996, pp. 41–46.

[3] Y. Furukawa and M. Abe, "Direct yaw moment control with estimating side-slip angle by using on-board-tire-model," in *Proc. 4th Int. Symp. Advanced Vehicle Control (AVEC)*, Nagoya, Japan, 1998, pp. 431–436.

[4] T. Furuya, Y. Toyoda, and Y. Hori, "Implementation of advanced adhesion control for electric vehicle," in *Proc. IEEE Workshop Advanced Motion Control (AMC)*, vol. 2, 1996, pp. 430–4356.

[5] F. Gustafsson, "Slip-based tire-road friction estimation," *Automatica*, vol. 33, no. 6, pp. 1087–1099, 1997.

[6] Y. Hori, Y. Toyoda, and Y. Tsuruoka, "Traction control of electric vehicle based on the estimation of road surface condition, basic experimental results using the test ev "UOT March"," *IEEE Trans. Ind. Applicat.*, vol. 34, pp. 1131–1138, Sept. Oct. 1998.

[7] N. Iwama *et al.*, "Active control of an automobile—Independent rear wheel torque control—," in *Trans. Soc. Instrum. Contr. Eng.*, vol. 28, 1992, pp. 844–853.

[8] C. Liu and H. Peng, "Road friction coefficient estimation for vehicle path prediction," *Veh. Syst. Dyn. Suppl.*, vol. 25, pp. 413–425, 1996.

[9] S. Motoyama *et al.*, "Effect of traction force distribution control on vehicle dynamics," in *Proc. Int. Symp. Advanced Vehicle Control (AVEC)*, 1992.

[10] T. Okano, C. Tai, T. Inoue, T. Uchida, S. Sakai, and Y. Hori, "Vehicle stability improvement based on MFC independently installed on 4 wheels—Basic experiments using 'UOT Electric March II'," in *Proc. PCC-Osaka*, 2002, CD-ROM.

[11] L. R. Ray, "Nonlinear tire force estimation and road friction identification: Simulation and experiments," *Automatica*, vol. 33, no. 10, pp. 1819–1833, 1997.

[12] H. Sado, S. Sakai, and Y. Hori, "Road condition estimation for traction control in electric vehicle," in *Proc. IEEE Int. Symp. Industrial Electronics*, Slovenia, 1999, pp. 973–978.

[13] S. Sakai and Y. Hori, "Robustified model matching control for motion control of electric vehicle," in *Proc. IEEE Workshop Advanced Motion Control*, 1998, pp. 574–579.

[14] S. Sakai, H. Sado, and Y. Hori, "Motion control in an electric vehicle with 4-independently driven in-wheel motors," *IEEE/ASME Trans. Mechatron.*, vol. 4, pp. 9–16, Mar. 1999.

[15] ——, "Novel skid avoidance method without vehicle chassis speed for electric vehicle," in *Proc. Int. Power Electronics Conf. (IPEC-2000)*, vol. 4, 2000, pp. 1979–1984.

[16] ——, "Novel wheel skid detection method for electric vehicles," in *Proc. 16th Electric Vehicle Symp. (EVS16)*, Beijing, China, 1999, p. 75.

[17] Y. Shibahata *et al.*, "The improvement of vehicle maneuverability by direct yaw moment control," *Proc. 1st Int. Symp. Advanced Vehicle Control (AVEC)*, no. 923081, 1992.

[18] S. Sakai and Y. Hori, "Advanced vehicle motion control of electric vehicle based on the fast motor torque response," in *Proc. 5th Int. Symp. Advanced Vehicle Control (AVEC)*, 2000, pp. 729–736.

[19] S. Sakai, H. Sado, and Y. Hori, "Novel skid detection method without vehicle chassis speed for electric vehicle," in *JSAE Rev.*, vol. 21, 2000, pp. 503–510.

[20] S. Sakai, T. Okano, C. Tai, T. Uchida, and Y. Hori, "4 wheel motored vehicle "The UOT March II"—Experimental EV for novel motion control studies—," in *Proc. First ISA/JEMIMA/SICE Joint Tech. Conf.*, 2001.

[21] ——, "Experimental studies on vehicle motion stabilization with 4 wheel motored EV," in *Proc. EVS-18*, 2001.

[22] S. K. Sul and S. J. Lee, "An integral battery charger for four-wheel drive electric vehicle," *IEEE Trans. Ind. Applicat.*, vol. 31, Sept./Oct. 1995.

[23] Y. Wang and M. Nagai, "Integrated control of four-wheel-steer and yaw moment to improve dynamic stability margin," in *Proc. 35th IEEE-CDC*, 1996, pp. 1783–1784.

[24] S. Yamazaki, T. Fujikawa, and I. Yamaguchi, "A study on braking and driving properties of automotive tires," *Trans. Soc. Automotive Eng. Jpn.*, vol. 23, no. 2, pp. 97–102, 1992.

[25] S. Yamazaki, T. Suzuki, and I. Yamaguchi, "An estimation method of hydroplaning phenomena of tire during traveling on wet road," in *Proc. JSAE Spring Conf.*, Yokohama, SE, Japan, 1999, pp. 5–8.

Yoichi Hori (S'81–M'83–SM'00) received the B.S., M.S., and Ph.D. degrees in electrical engineering from The University of Tokyo, Tokyo, Japan, in 1978, 1980, and 1983, respectively.

In 1983, he joined the Department of Electrical Engineering, The University of Tokyo, as a Research Associate. He later became an Assistant Professor, an Associate Professor, and, in 2000, a Professor. In 2002, he moved to the Institute of Industrial Science at The University of Tokyo, as a Professor in the Information and System Division, Electrical Control System Engineering. During 1991–1992, he was a Visiting Researcher at the University of California, Berkeley. His research fields are control theory and its industrial applications to motion control, mechatronics, robotics, electric vehicles, etc.

Prof. Hori has been the Treasurer of the IEEE Japan Council and Tokyo Section since 2001. He is currently the Vice President of the Industry Applications Society of the Institute of Electrical Engineers of Japan (IEEJ). He was the winner of the 1992 ROBOMEC Award of the Robotics and Mechatronics Society of the Japan Society of Mechanical Engineers (JSME), the 1993 Third Prize in the IEEE-IECON'93 Best Paper Competition, the Best Transactions Paper Award from the IEEE TRANSACTIONS ON INDUSTRIAL ELECTRONICS in 1993, the 2000 Best Transactions Paper Award from the IEEJ. He was one of nine finalists for the Poster Paper Prize at the 1996 IFAC World Congress, and a finalist in the Best Vision Paper Competition at the 2001 IEEE-ICRA. He also received a Technical Committee Prize Award from the Industrial Drives Committee of the IEEE Industry Applications Society in 2001. He is a Member of the IEEJ, Society of Instrument and Control Engineers, Robotics Society of Japan, JSME, and Society of Automotive Engineers of Japan.